Chapter 11
Core–Shell Structured Nanomaterials for High-Performance Dielectric Applications

Anupam Sahoo, Sangita Kumari Swain, and Sukanta Kumar Swain

Abstract Green energy is a relatively new kind of energy that is gaining considerable interest from nations all over the globe as a solution to the problem of environmental pollution on a global scale as well as the current energy crisis (Luo et al. in Adv Energy Mater 9(5):1803204, 2019 [1], Wang et al. in J Mater Chem A 8(22):11124–11132, 2020 [2], Wang et al. in Nano Energy 78:105247, 2020 [3], Zheng et al. in Compos Sci Technol 222:109379, 2022 [4]). Owing to numerous applications in the electronic and electrical industries, such as transistors, actuators, and capacitors, dielectric materials having low dielectric loss and high dielectric constant have gained growing consideration in recent years (Zheng et al. in Compos Sci Technol 222:109379, 2022 [4], He et al. in Compos A Appl Sci Manuf 93:137–143, 2017 [5], Huang and Jiang in Adv Mater 27(3):546–554, 2015 [6], Wang et al. in IEEE Trans Dielectr Electr Insul 17(4):1036–1042, 2010 [7]). In this chapter, various types of core–shell nanoparticles are discussed for high-performance dielectric applications.

Keywords Core–shell nanoparticles · Dielectric materials · Polymer nanocomposites · High-k materials

11.1 Introduction

High dielectric constant materials (high-k) possess various implications in organic thin-film electroluminescent devices [8], organic field effect transistors (OFETs) [9–11], actuators, and [12, 13] energy storage devices [14–16], and electrical stress

A. Sahoo (✉)
Department of Chemistry, Sri Krushna Chandra Gajapati (Autonomous) College, Paralakhemundi, Odisha, India
e-mail: anupamchem0@gmail.com

S. K. Swain
Centre of Excellence, Berhampur University, Berhampur, Odisha, India

S. K. Swain
Department of ECE, Indian Institute of Information Technology, Ranchi, Jharkhand, India

S. Moharana et al. (eds.), *Emerging Nanodielectric Materials for Energy Storage*, Nanostructure Science and Technology, https://doi.org/10.1007/978-3-031-40938-7_11

control applications[17–19]. High-k materials have the ability to significantly lower the surface electric stress and maintain it at a level that is lower than the breakdown strength of air that may finally lead to the elimination of the surface discharge. A seamless high-k material has the characteristics such as high dielectric constant, high breakdown strength, minimal dielectric loss, and superior processability. These are the general features of an ideal high-k material. In general, polymers based on organic molecules have a high breakdown strength and are simple to produce, however the vast majority of organic polymers have disadvantage of low dielectric constant, e.g., around 2.0–5.0. Despite the fact that many have very high dielectric constants, the dielectric loss of these materials is often rather considerable, especially when subjected to strong electric fields [20]. In addition to having enormous dielectric constants that range from ~1000 to 10,000, dielectric ceramics like $BaTiO_3$ have lower breakdown strengths and/or substantial dielectric loss [21]. Additionally, their lack of flexibility and low processability severely restrict their use. In general, it is challenging to discover a single material that combines all the required qualities for real-world applications. Therefore, it may be anticipated that combining the benefits of ceramics with polymers would be a successful strategy for developing new high-k materials.

When compared with microparticles, the interlinked area that polymer material has with nanoparticles is much higher. Nanoparticles impart larger interconnected areas in comparison with micro-sized particles, with the polymer nanocomposites. As a result, nanoparticles are the potential materials that exhibit significantly higher polarization levels, mechanical enhancements, and breakdown strength. Additionally, they provide more opportunities to tune and optimize the characteristics of the polymer matrix. Further, the smaller size of nanomaterials makes them feasible to lower the fabrication dimensions of devices based on polymer nanocomposites. This is a feature that is of the utmost significance for the ongoing process of shrinking the size of electronic devices. In the case of embedded planar capacitors, for instance, the dielectric film must be very thin in order to provide a higher capacitance; normally, this is accomplished using films on the micrometer scale. When measured on this scale, an enhancement in the size of the high-k particles from 100 nm to 2 μm results in a considerable reduction in the capacitance density of polymer composite films [22]. These exciting factors make nanoparticles most significant for the development of high-k dielectric materials.

Although the incorporation of nanoparticles into the design of high-k polymer composites has a number of opportunities for improvement, the realization of high-performance nanocomposites presents a number of obstacles. The synthesis of homogenously dispersed nanoparticles and the tuning of interfaces between polymer and nanoparticle are typical examples of existing problems. Both of these factors play significant roles in producing appropriate electrical and other characteristics. Surface modification of nanoparticles by coupling agents [18], hydroxylation [23], surfactants, phosphoric acids, and other organic compounds [24–26] has been extensively employed to enhance the performance of polymer nanocomposites to achieve a high-k material. However, these approaches still have certain drawbacks in terms of achieving the complete potential of a high-performance polymer matrix. This is due

to the fact that the surface modifiers themselves do not often exhibit huge participation in the enhancement of the dielectric characteristics of the nanocomposites.

Over the past few years, considerable efforts has been invested in the synthesis and design of core–shell nanoparticles, with the goal of realizing the full potential that nanoparticles have to offer in terms of improving the characteristics of polymer nanocomposites. Figure 11.1 provides many generic ways for manufacturing high-k polymer nanocomposites utilizing core–shell methodologies. As an example, this figure uses $BaTiO_3$ as its subject. These approaches may be broken down into the following four categories:

(i) Core–shell nanoparticles that have been fabricated by "grafting from" [27–29]
(ii) Core–shell nanoparticles that have been fabricated by "grafting to" [30–33]
(iii) The use of organic–inorganic based core–shell nanoparticles as filler materials [34, 35] and
(iv) The use of other varieties of core–shell nanoparticles as filler materials [36–39].

This chapter focuses mostly on reviewing these developing approaches. In order to successfully use high-k polymer nanocomposites, it is essential to strike an appropriate balance between the dielectric loss, dielectric constant, and breakdown strength[40–42]. For this reason, a focus is made by virtue of core–shell techniques in attaining lower dielectric loss and strong breakdown strength while simultaneously preserving the high dielectric constant of the various nanocomposite

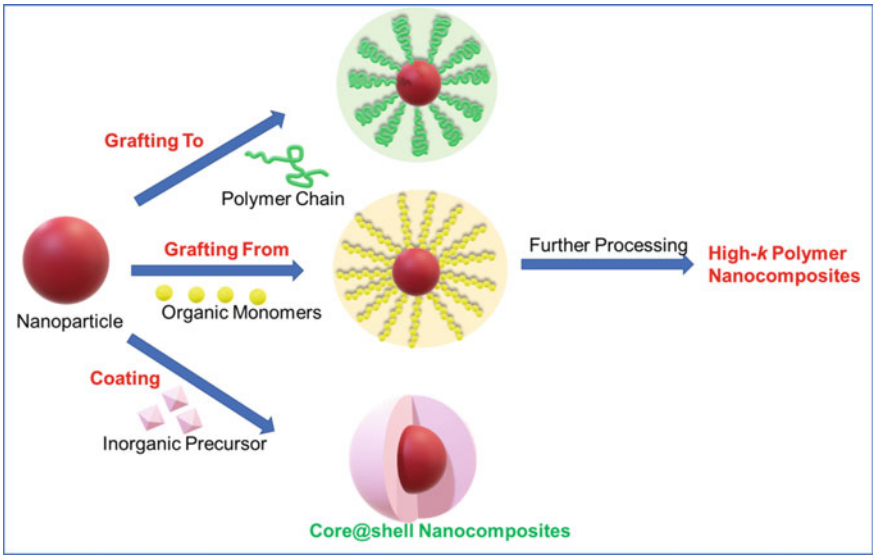

Fig. 11.1 Methods adopted for the synthesis of core–shell nanoparticles for high-k polymer nanocomposite matrix

matrices. However, it is important to know about the advantages and classes of core–shell nanoparticles. The following section describes a brief idea about core–shell nanoparticles.

11.2 Classification of Core–Shell Nanomaterials

Nanoparticles may be classified into simple, core/shell, and composite categories, depending on whether they are composed of a single substance or many components. In general, nanoparticles that are classified as simple are constructed using just a single kind of material. On the other hand, particles classified as composite or core/shell are made up of two or more types of materials. The core–shell type of nanoparticles may be broadly characterized as nanoparticles that consist of an inner core material and an exterior shell material (outer layer material). These may be made up of a broad variety of distinct combinations that are interacting closely with one another, such as components that are organic/organic, organic/inorganic, inorganic/organic, or inorganic/organic. The final application and purpose often have a significant impact on the material that is selected to function as the shell of the core–shell nanoparticle. Figure 11.2 provides a schematic representation of many distinct types of core–shell nanoparticles. Concentric spherical core/shell nanoparticles are considered to be the most common kind of nanoparticle (Fig. 11.2a), which consists of a basic spherical core particle that is entirely covered by a shell made of a different substance. Due to the fact that they each possess their own unique set of characteristics, various core/shell nanoparticles have also sparked a significant amount of research interest. When a core is not spherical, as illustrated in Fig. 11.2b, different shaped core/shell nanoparticles will often occur.

Multiple core core–shell particles may be created, as shown in Fig. 11.2c when a single layer of shell material is deposited concurrently over a large number of relatively small core particles. This can result in the formation of multiple core/shell particles. Nanoshells are shown as having alternating coatings of dielectric core material and metal shell material onto each other in Fig. 11.2d. These nanoshells are concentric in nature. These nanoshells have an A/B/A structure configuration. In this structure, nanoscale spacer layers made of dielectric material are employed to separate concentric layers of metallic material. These sorts of nanoparticles are known as nanomaterial or multi-layered metal-dielectric nanostructures. Such materials possess unique plasmonic properties.

The plasmonic features of these types of particles are the major reason for their significance. After applying a bilayer coating of the core material and then using the proper procedure to remove the first layer, it is also feasible to fabricate a movable core particle that is contained inside a hollow spherical shell material (shown in Fig. 11.2e). This can be done after a double-layer coating of the core material [43].

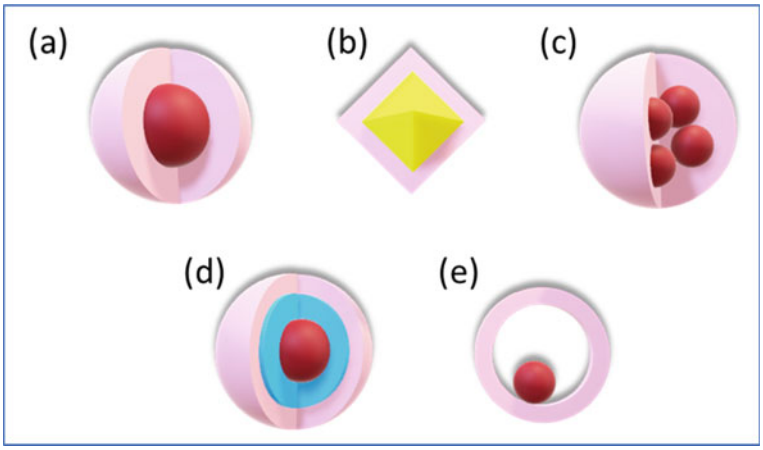

Fig. 11.2 Various types of core–shell nanoparticles; **a** Spherical, **b** Hexagonal, **c** Multicore single shell, **d** Multi-layered nanomaterial, **e** Movable core in the shell

11.3 Approaches for the Development of Core–Shell Polymer Nanocomposites with High-k

11.3.1 Core–Shell Nanoparticles Produced Using the "Grafting-From" Technique

This technique is based on the in situ polymerization of monomers on the surfaces of nanoparticles that have been functionalized with an initiator. This results in the production of nanocomposites. The incorporation of an adequate number of starting sites onto the surfaces of the nanoparticles is the essential component of this technique. The controlled or live radical polymerization approach, which includes techniques such as

a. Reversible addition-fragmentation chain transfer polymerization (RAFT)
b. Atom transfer radical polymerization (ATRP),

These are the potent "grafting from" methods. These methods offer many benefits as follows [27–29, 35].

(i) The shell layer may be formed as a matrix to form highly stable core–shell materials with high-quality and highly filled materials free of voids, pores, and defects.
(ii) The nanoparticle aggregation has been prevented by the outer layer (shell) of the core material.
(iii) The feed ratio of the monomer and the functionalized initiator nanoparticles may be modified to change the nanoparticle concentration.

(iv) Any polymer chains are firmly attached to the surfaces of the nanoparticles, creating a sturdy nanoparticle/matrix composite with an intact interface.
(v) A wide variety of monomers may be converted into polymers.

Jiang and Huang utilized polystyrene (PS) and poly (methyl methacrylate) [PMMA] nanocomposites and adopted RAFT and ATRP to synthesize high-k core–shell PS@$BaTiO_3$ and PMMA@$BaTiO_3$ nanoparticles correspondingly [28, 29]. The schematic representation has been shown in Fig. 11.3. In both these types of nanoparticles homogeneous dispersion has been observed. The dielectric constant was increased from 2.80 to 24 with the 48 vol% $BaTiO_3$in PS@$BaTiO_3$ nanocomposite while compared with pure PS. The dielectric loss was mostly as low as pure PS. The result depicted that the dielectric loss and dielectric constant remained stable over a wide scale of frequencies. This result provided the potential for this material to be used in various functional devices and exhibits a stable and insensitive operation with varying frequencies.

Electrical vehicles, consumer electronics pulse-power systems, and electric grids make extensive use of capacitors made from biaxially oriented polypropylene (BOPP) film because of the unique blend of properties that it possesses. These properties include high breakdown strength, low energy loss, and low-capacity loss even under conditions like high sealability, frequencies, flexibility, and lightweight. However, due to the lower dielectric constant of polypropylene (PP), the use of BOPP is restricted from being utilized in potential future applications that may call

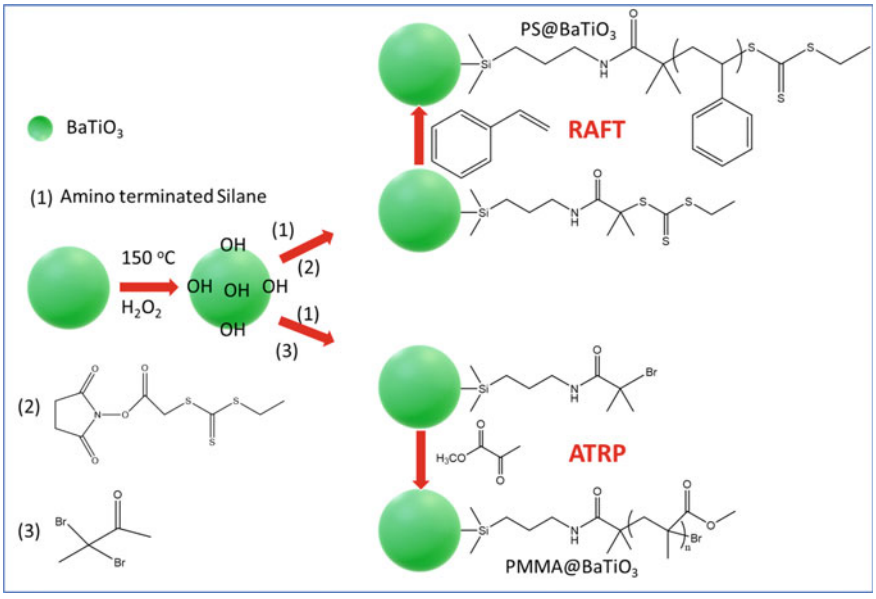

Fig. 11.3 Schematic representation of the preparation procedure for high-k PMMA and PS nanomaterials by RAFT and ATRP polymerization techniques, correspondingly

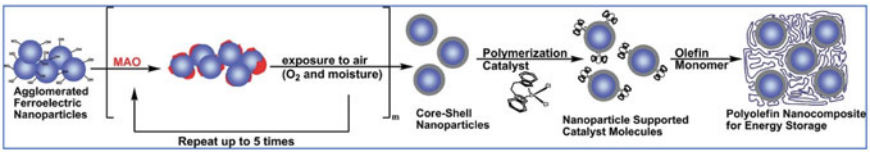

Fig. 11.4 Schematic presentation of synthetic routes of PP core–shell nanocomposite matrix [32]. Reproduced with permission from Ref. [32]. Copyright 2010, American Chemical Society

for the speedy transmission of significant amounts of energy. An efficient approach for the fabrication of PP-based high-k and low-loss nanocomposites was reported to have been developed by the Marks research group in the year 2007 [32, 44–47]. In this procedure, initially the nanoparticles (e.g., Al, TiO_2, $SrTiO_3$, $BaTiO_3$, MgO, ZrO_2, and $Ba_{0.5}Sr_{0.5}TiO_3$) were treated with a co-catalyst methylaluminoxane (MAO) which enabled the formation of Al-O bond with covalent character (Fig. 11.4).

Further, the nanoparticles that had been treated with MAO were put through a reaction with a catalyst acethylenebisindenyl zirconium chloride ($EBIZrCl_2$) for metallocene olefin polymerization. The surface functionalization of MAO on nanoparticles utilizing $EBIZrCl_2$ led to the development of species active for polymerization, being anchored on the surfaces of the nanoparticles. These polymerization-active species had the ability to initiate the in situ propylene polymerization, which ultimately resulted in the production of isotactic PP (^{iso}PP) nanocomposites. In comparison with pure PP, the ^{iso}PP nanocomposites that were synthesized, displayed significantly increased energy storage capacity as a result of their increased dielectric constant, as well as their suitably high breakdown strength.

Even though this approach only works with a small number of monomers, it offers a number of special advantages:

(i) The production of nanocomposites is quite feasible.
(ii) Large local hydrostatic pressures caused by the propagating polyolefin chains from the active catalyst centers may prevent nanoparticle agglomeration in the final nanocomposites.

Most significantly, this technology offers a practical approach to reducing the amount of electrical mismatch that exists between the matrix and the nanoparticles. Specifically, the nanoparticles are covered with a material (Al_2O_3) having a dielectric constant that is lower than that of the nanoparticles but higher than that of the matrix themselves. It is worth noting that the large dielectric constant mismatch is the primary cause of the reduction in the breakdown strength of high-k polymer composites. Keeping this in mind, the incorporation of Al_2O_3 may prove to be advantageous in preserving the high breakdown strength of nanomaterials. In specifically, Al-^{iso} PP nanocomposites show a remarkable breakdown strength[47]. According to the findings that were published by Marks, even at a high concentration (12.4 vol%) of metal nanoparticles, the Al-^{iso} PP composites exhibit a high breakdown strength of almost 80 MV m^{-1}. Even when the particle concentration is well below the percolation threshold, polymer composites filled with conductive particles typically display

a very lower breakdown strength as a consequence of the electrical conduction that occurs as a result of inter-particle tunneling. This is the case even when the particle concentration is extremely low [48]. In this case, the ^{iso}PP nanocomposite matrix having a high amount of Al nanoparticles shows high breakdown strength. This may be due to the surface modification by Al_2O_3 layer, which hinders the tunneling current among particles. This is the case because these nanocomposites have a higher percentage ratio of Al nanoparticles in the composite.

11.3.2 Core–Shell Structure Fabricated Using the "Grafting-To" Method

This technique includes the production of nanomaterials by grafting the pre-synthesized polymers onto the surface of the nanoparticles. This grafting takes place as a result of an interaction between the functional groups on the surfaces of nanoparticles and the polymer end-groups. In contrast to the "grafting from" method, the "grafting to" method enables us to exercise greater command over the molecular composition as well as the molecular mass of the polymer molecules. This gives us the ability to tailor the ultimate nanocomposites to achieve the desired level of performance.

Click chemistry is a universal approach that can be utilized to join reactants. It possesses the benefits of insensitivity to solvents, high efficacy, and mild reaction parameters. Click chemistry was developed in the 1970s. As a result, click reactions are an adaptable approach for the grafting of polymer molecules to the surfaces of nanoparticles. Vaia and Tchoul et al. have used a Cu(I)-catalyzed azide-alkyne click reaction (CuAAC) to create a sequence of core–shell PS@TiO_2 nanocomposite matrix [30].

The core–shell PS nanocomposites having 27 vol% TiO_2 had a dielectric constant of 6.4 at 1000 Hz, while the dielectric loss tangent was as low as 0.625%. The nanocomposites were made with 100 kg mol^{-1} of PS. In order to obtain high carrier mobility and low leakage current in thin-film-transistors based on organic semiconductors, the composite can be utilized as the gate dielectric in these devices [31].

Due to its high complexation with azides and triazoles, the CuBr catalyst utilized in the CuAAC process cannot be readily recovered from the nanocomposites. This strong complexation has the potential to create strong frequency-dependent dielectric characteristics as well as substantial dielectric loss. In contrast to the CuAAC reaction process, the thiol-ene click chemistry is very effective and does not produce any undesirable by-products. Further, it does not need the transition metals for the catalytic process to progress. The fabrication of core–shell polymer nanocomposites is made significantly easier by the use of the thiol-ene click reaction. Utilizing thiol-ene reaction method, Huang and Jiang developed polymer@$BaTiO_3$ nanocomposite matrices. The preparation procedure is depicted in Fig. 11.5a [49].

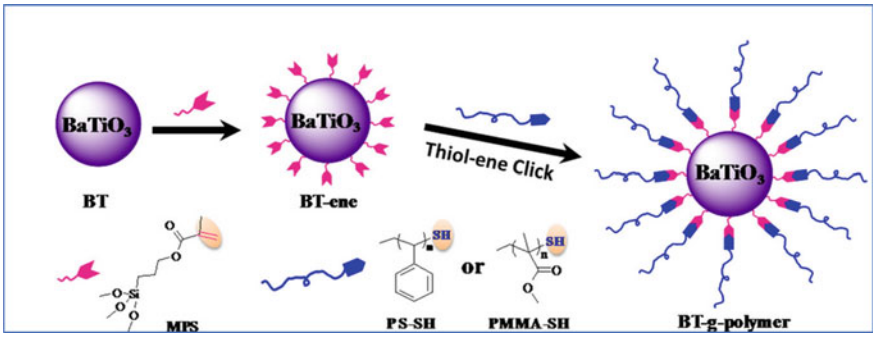

Fig. 11.5 Schematic presentation of synthetic procedure for PS@$BaTiO_3$ and PMMA@$BaTiO_3$ nanomaterials utilizing the thiol-ene click reaction [49]. Adopted with permission from Ref. [49] copyright@2014, American Chemical Society

By employing the thiol-ene click reaction macromolecules are grafted onto vinyl-functionalized $BaTiO_3$nanoparticle surface to synthesize core–shell polymer@$BaTiO_3$ nanoparticles. Using RAFT polymerization, initially, thiol-ended PMMA or PS macromolecules of various molecular mass were developed. Except for extremely low frequencies, the nanocomposites displayed a considerably improved dielectric constant, although the dielectric loss remained just as low when compared with pure polymer. This investigation also demonstrated that the dielectric properties of the polymer@$BaTiO_3$core–shellcomposite depended upon two factors. These factors include the grafting density of the core–shell structured nanoparticles and the molecular mass of the polymer chains, particularly at low frequencies. In particular, the dielectric loss was shown to be related to the molecular mass of the polymer molecules. High molecular mass polymer chains frequently have a propensity to cause poor grafting density and hence show a significant dielectric loss in nanocomposites [50].

Except for click reaction, the technique of producing core–shell structured high-k nanocomposites may make use of any alternative reaction to facilitate a linkage between nanoparticle surface and organic molecule chains. Maliakal et al. are able to affix oleic acid-terminated TiO_2 nanoparticle surfaces and phosphonate end-functionalized PS and effectively create core–shell high-k PS@TiO_2 nanocomposite dielectrics. This was done in an effort to find organic thin-film semiconductor transistors with high-k [31].

When the volume percentage of TiO_2 reached 18.2% the nanocomposite matrix exhibited a high dielectric constant (9.4), and the transistor that was produced demonstrated good mobility, which was desirable. Kim and Jung synthesized core–shell nanomaterials by surrounding $BaTiO_3$ with a PS-based copolymer. The name of the copolymer was polystyrene-block-poly (styrene-co-vinylbenzylchloride) [PS-b-PSVBC]. This resulted in a novel core–shell material in which the positively charged PSVBC was protected by the negatively charged PS shell. In such a case, the charged PSVBC shell resulted in improvements in the dielectric constant, while the PS shell

operated to lower the amount of leakage current and minimize the formation of breakdown channels. Both effects were achieved via the combined efforts of the two shells. The increase in the dielectric constant may be traced back to the primary reason, which is the increased interfacial polarization that can be found between the PSVBC shell and the PS shell. In conclusion, the shielding of the PS shell on the charged PSVBC shell is responsible for the decrease in leakage currents as well as the rise in breakdown strength. The nanocomposite materials demonstrated a substantially enhanced energy storage density, and the PS-b-PSVBC composite matrix composed of 75 weight percent $BaTiO_3$ was discovered to have the greatest energy density determined theoretically. The energy density was found to be 9.7 J cm^{-3}. The nanocomposites also showed a significant reduction in the amount of space required to store the energy [33].

When it comes to the preparation of high-k nanocomposites on a large scale, the use of polymers that are readily available on the market as shells is the more appealing option. In recent work, Huang and Jiang generated polymer@$BaTiO_3$core–shell nanocomposites by adopting the "grafting to" technique with high-k. They accomplished this by employing poly (vinylidene fluoride-co-hexafluoropropylene) [PVDF-HFP] functionalized with commercially available poly (glycidyl methacrylate) [PGMA] [51]. The PGMA-functionalized PVDF-HFP generated a strong and durable layer on the surface of $BaTiO_3$, providing a homogeneous distribution of $BaTiO_3$ in PVDF-HFP matrix. Additionally, the energy density and dielectric constant of the nanocomposite matrix improved with increasing $BaTiO_3$ concentration, although the dielectric loss dropped moderately. This was seen despite the fact that the dielectric loss increased to some extent.

11.3.3 Nanoparticles Comprised of an Organic Core Surrounded by an Inorganic Shell Used as Fillers

This method refers to the synthesis of polymer matrix by inserting core–shell inorganic–organic nanomaterial into a nanocomposite, analogous to the usual solution-mixing and melt-mixing processes for preparing composites. The ability to accurately control the concentration of inorganic nanoparticles within the nanocomposites as well as the qualities that are closely connected with the nanoparticle concentration is one of the most significant benefits of this technology. The importance of this method lies in the fact that it enables an individual to gain a basic understanding of the function exhibited by the interface in determining the electrical characteristics of the nanocomposite matrix. Huang and co-worker explored the effect of matrix/shell physical interface interactions on the dielectric properties of nanocomposites composed of fluoro-polymer@$BaTiO_3$ nanoparticles and ferroelectric polymers [35]. They started with preparing core–shell fluoro-polymer@$BaTiO_3$ nanoparticles, which not only had differing thicknesses of polymer shell but also had different molecular structures. This was accomplished by inserting two different kinds of monomers based on

fluoroalkyl acrylate by RAFT polymerization. These are specifically, trifluoroethyl acrylate (TFEA), and 1H, 1H, 2H, 2H-heptadecafluorodecyl acrylate (HFDA). The nanocomposites were made by first combining the fluoro-polymer with the $BaTiO_3$ nanoparticles, and then adding the PVDF-HFP. The authors discovered that the shell structure of the fluoro-polymer@$BaTiO_3$ was closely connected with the dielectric characteristics and energy storage capacity of the nanocomposite matrix. The authors hypothesized that the ordered chain structure of PHFDA led to lower inter-chain interactions and lower chain mobility between PHFDA@$BaTiO_3$ and the PVDF-HFP composite matrix, whereas the irregular arrangement of the chain structure of PTFEA led to higher inter-chain interactions and higher chain mobility between PTFEA@$BaTiO_3$ and the PVDF-HFP composite matrix. This led to a more robust suppression of the space charge. Because of this, the PTFEA@$BaTiO_3$ nanocomposites were able to attain a reduced dielectric loss, a higher breakdown strength, and a greater capacity for energy storage. The effect that the shell/matrix chemical interaction plays (also known as interfacial bonding) in determining the dielectric characteristics of high-k polymer nanocomposites was another aspect that Huang and Jiang looked at. They did this by comparing the dielectric characteristics of single-core double-shell nanocomposite matrix (NC I) and single-core single-shell nanoparticle-filled nanocomposites (NC II). In this case, the matrix of NC II and the outer shell of NC I shared an identical chemical structure [52].

Functionalizing hyperbranched aromatic polyamides (HBP) onto the surfaces of the $BaTiO_3$ nanoparticles was the initial step in the process of making single-core single-shell nanoparticles, which they referred to as HBP@$BaTiO_3$. Then, they grew PMMA on the surface of HBP@$BaTiO_3$ nanoparticles in order to construct nanocomposite I (also known as PMMA@HBP@$BaTiO_3$). This was done by using ATRP. The nanocomposite known as nanocomposite II (PMMA/HBP@$BaTiO_3$) was created by combining core–shell HBP@$BaTiO_3$ nanocomposite with PMMA [52].

Both nanocomposites displayed a nanoparticle dispersion that was homogeneous across their structures and strong adhesion between their interfaces. Dielectric analysis, on the other hand, revealed that the two types of nanocomposites displayed significantly distinct sets of properties. The PMMA@HBP@$BaTiO_3$ nanomaterials show high electrical insulation. This exhibited low electrical conductivity at low frequencies. Electrical conductivities were substantially frequency dependent, whereas dielectric properties were only mildly frequency dependent. Because of their high dielectric constant, these materials are particularly appealing for use in applications involving energy storage and gate dielectrics. On the other hand, the highly loaded PMMA/HBP@$BaTiO_3$ nanocomposites exhibited dielectric characteristics that were comparable with those of percolative composites.

To be more specific, the electrical conductivity of the nanocomposites was not affected by frequency. However, the dielectric constant and dielectric loss of the nanocomposite exhibited a significant increase at low frequencies, while simultaneously demonstrating a rapid decrease as the frequency was increased. In spite of the extremely high dielectric constant that was attained, the PMMA/HBP@$BaTiO_3$ nanocomposites are not desirable for use in any power energy storage or dielectric

application. This is because the nanocomposites have substantial electrical conductivities and dielectric loss. In a different study, Huang and Jiang created mixes of fluoro-tripolymer and HBP@$BaTiO_3$. It was observed that the core–shell HBP@$BaTiO_3$ nanoparticles were not compatible with the fluoro-tripolymer matrix [53].

The researchers investigated that when the composites were subjected to relatively high concentrations of HBP@$BaTiO_3$ (i.e., concentrations that were more than 20% by volume), the composites started to demonstrate properties of dielectric materials that were comparable with those of percolative nanocomposites. According to the findings of the two observations that were just discussed, the establishment of interfacial interaction is typically the most important feature that plays a role in realizing required dielectric characteristics in composites when the matrix and the introduced inclusion have a significant difference in their electrical conductivity. In the instance of single-core double-shell nanomaterials, the inner shell was covalently bound to the outer shell. The outer shell was capable to prevent the passage of charge carriers by acting as a shield on the charge-rich inner shell. This caused poor interfacial polarization and a lower leakage current density, which in turn enhanced the dielectric properties of the nanocomposites and resulted in a low dielectric loss.

A number of the core–shell polymer@$BaTiO_3$ documented in the literature still now, have been based on commercially accessible $BaTiO_3$ nanoparticles, which is a technique that is quite viable and might potentially save time. However, these approaches are not able to control the size of the nanoparticles, and as a result, their electrical properties are size-dependent. More recently, the research team led by Lin presented an exciting technique to manufacture core–shell nanocomposites, comprising the core–shell polymer@$BaTiO_3$ [54, 55]. They started by preparing star-like gigantic molecules, as shown in Fig. 11.6. For this purpose, poly (acrylic-acid)-block-polystyrene (PAA-b-PS) was generated from a core comprised of cyclodextrin using ATRP and process of hydrolysis. Further, they added the inorganic precursor, and by selecting the appropriate solvent, they were able to force the precursor to concentrate in the hydrophilic core poly (acrylic-acid) of the PAA-b-PS. Condensation at elevated temperatures finally produced single-crystalline $BaTiO_3$ nanoparticles that were the same size as that of the PAA core. By utilizing this method, it was possible to regulate the size of the crystalline $BaTiO_3$ nanoparticles by adjusting the core size of the PAA. It was found that two different types of core–shell nanoparticles with varying $BaTiO_3$ sizes (11 and 27 nm) were effectively synthesized. These core–shell nanoparticles resulted in high dielectric constants than that of formerly published core–shell nanomaterials. It was primarily because of the higher size (approximately 50–140 nm) of commercially accessible $BaTiO_3$ nanoparticles [34, 54].

It is interesting to note that the core–shell nanoparticles are also known to be used as fillers during the synthesis of high-k polymer nanocomposites based on deblock copolymer (PS-b-PMMA). PS@$BaTiO_3$ was injected selectively into the cylindrical PS nanodomains in PS-b-PMMA, yielding in nanocomposites with vertically oriented PS nanocylinders filled with PS@$BaTiO_3$. This is in contrast to the nanocomposites that were created using conventional mixing techniques, in which

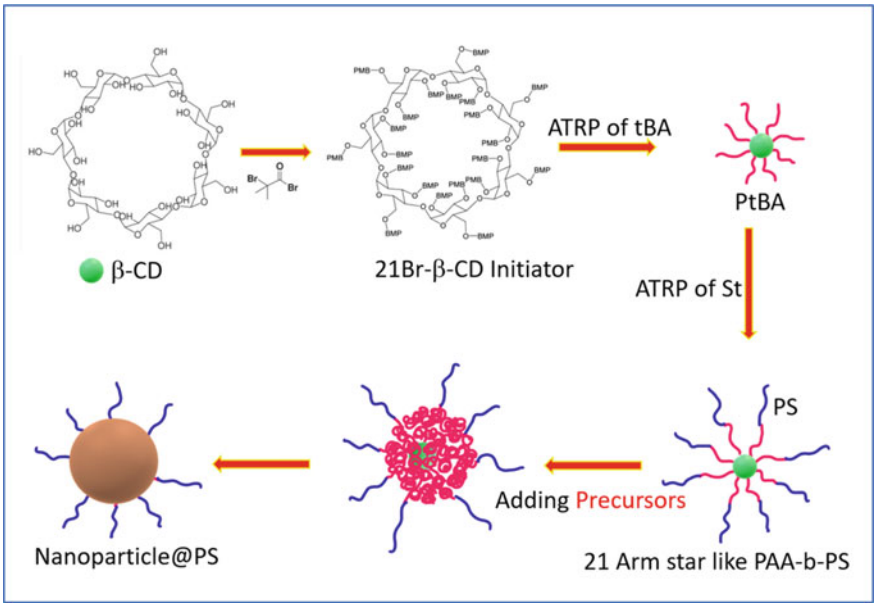

Fig. 11.6 Scheme displaying synthetic approach of PS@$BaTiO_3$ core–shell nanocomposite

the nanomaterials were arbitrarily dispersed throughout a polymer matrix. The PS-b-PMMA/PS@$BaTiO_3$ nanocomposites exhibited high dielectric constants (greater than 18) independent of frequency. Additionally, a negligible dielectric loss was observed even at a high-frequency range of 2–15 GHz. These nanocomposites also showed tremendous potential for dielectric and energy storage applications[34].

11.3.4 Core–Shell Nanoparticles of Other Types as Fillers

In addition to core–shell structured inorganic–organic nanoparticles, to create high-k polymer nanocomposites, different varieties of core–shell nanocomposites have also been utilized as filler materials. These nanoparticles include inorganic-inorganic (e.g., SiO_2 @ $BaTiO_3$ and TiO_2@$BaTiO_3$) [38, 56], organic-organic (e.g., PDVB@PANI, and poly divinyl benene@polyaniline) hybrids, metal-inorganic (e.g., TiO_2 @ Ag), and Al_2O_3 @Al [36, 39], and metal–organic (e.g., C@Ag) [37, 57, 58]. The core–shell structured TiO_2 @ $BaTiO_3$ nanoparticles as well as the associated PVDF nanocomposites were synthesized by Yao and Rahimabady [56]. They made a startling discovery when they compared the dielectric characteristics of the PVDF/TiO_2@$BaTiO_3$ nanocomposites with those of the PVDF/$BaTiO_3$ nanocomposites: the PVDF/TiO_2 @$BaTiO_3$ nanocomposites exhibited a considerable improvement. Specifically, the PVDF/TiO_2 @$BaTiO_3$ nanocomposites exhibited an increase in

both the dielectric constant and the breakdown strength. Discharged energy density of the nanocomposite with 30 vol% TiO_2 @$BaTiO_3$ was 12.2 J cm^{-3} at 340 MV m^{-1}, which is almost three times as high as the discharged energy density of pure PVDF (4.1 J cm^{-3}). In polymer nanocomposites containing high-k particles, the large increase in dielectric constants is often achieved at the price of a reduction in breakdown strength. This is a conclusion that has been widely accepted based on research. Considering this interpretation, the findings of Yao and Rahimabady's study provide a significant piece of the puzzle necessary to reconcile this well-known discrepancy. The insertion of a TiO_2 layer, which resulted in a reduction in the local electric field distortion, was credited by the authors as the cause of the improvement in dielectric performance. The "buffer layer" hypothesis that had been developed by the Marks group is basically compatible with this finding. Wong and Xu are considered to be pioneers in the fabrication of core–shell structured Al_2O_3@Al nanoparticles for use in low-loss, high-k polymer nanocomposites[39].

It has been claimed that the dielectric constant may reach the highest value as 60 when the proportion of Al nanoparticles (about 100 nm in size) in the material is 50 weight percent, while the dielectric loss can reach a lower value of 0.02. The Al core which is electrically conductive causes a rise in electric field strength inside the polymer nanocomposite, which adds to a rise in the dielectric constant of nanocomposite matrix. As a consequence of the shielding Al_2O_3 layer that is located surrounding the Al core, electron transport between the Al nanoparticles is restricted, which in turn results in a minimal dielectric loss. Since Ag is an excellent electrical conductor, Ag-filled polymer composites function as conventional percolation systems. When the Ag nanoparticle loading is far below the percolation threshold in these systems, the dielectric constant of the composites grows slowly, and when it is close to the percolation threshold, it increases quickly. Since Ag is an excellent electrical conductor, Ag-filled polymer composites may function as characteristic percolation systems. After passing the percolation threshold, the composites eventually become electrically conductive, and after that, there is a sudden drop in the dielectric constant [59].

The creation of conductive routes between neighboring Ag nanoparticles is inhibited after the Ag nanoparticles have been enclosed by an insulating polymer shell. Additionally, the tunneling currents between neighboring Ag nanoparticles decrease as the shell thickness increases. Nanocomposite with an Ag core encapsulated by an insulating shell behave as insulating material even a considerable amount of Ag present after the shell width reaches a threshold value at which the tunneling current reduces to a minimal value. In this scenario, the nanocomposites will demonstrate both a high dielectric constant as well as a low dielectric loss at the same time. When the concentration of Ag nanoparticles was higher than 20 vol%, Shen and Nan discovered that the dielectric constant increased by more than two times in magnitude when the epoxy nanocomposite is filled with core–shellC@Ag nanoparticles as fillers. On the other hand, a little enhancement (i.e., from 2 to 4%) in the dielectric loss tangent was observed [37, 57].

Additionally, it is important to note that the shell thickness has an effect on the dielectric characteristics of the epoxy/C@Ag nanocomposites and that this effect

may be modified. Coulomb blockade and quantum confinement effects may take place if the diameter of a nanocrystal is shrunk to a size that is sufficiently small [60]. In this scenario, a metallic particle may acquire insulating properties against electrical current. In addition, there will be a restriction placed on the movement of electrons from one particle to its adjacent particle. In this scenario, one may make use of the coulomb blockade effects and quantum confinement of ultra-small metal nanomaterials in order to reduce the amount of leakage current and to improve the breakdown strength of nanocomposites. Based on this concept, Huang and Xie discovered that in contrast with $BaTiO_3$ nanomaterials, nanocomposite matrix packed with $BaTiO_3$ decorated with ultra-small Ag (such as Ag@$BaTiO_3$) hybrid nanoparticles had increased breakdown strength and lower dielectric loss [61]. Scientists inferred that the presence of coulomb-blockade effect in Ag@$BaTiO_3$ nanocomposites based on the dramatically reduced electrical conductivities of the nanocomposite. Core–shell nanoparticles that are based on inorganic and metal cores often have a high density, which might cause the target devices to become unnecessarily heavy. The use of completely organic fillers is encouraged as a means of lowering the device's overall weight while keeping the device's functioning intact. Opris and Molberg developed high-k poly diomethyl siloxane (PDMS) nanomaterials by utilizing polyaniline functionalized poly divinyl benzene (PDVB@PANI) core–shell particles [58].

Surprisingly, when dielectric constant PDMS/PDVB@PANI composites were compared with pure PDMS, an enhancement in dielectric constant was observed, however, exhibited a breakdown strength that was equivalent to that of pure PDMS. For instance, the dielectric constant rose from 2.3 for pure PDMS to 7.6 for composites containing 31.7% PDVB@PANI nanoparticles at 100 Hz, whereas the breakdown strength of the composites only exhibited a minor drop (going from 66.1 to 64.1 V m^{-1}) throughout this same time period.

Strawberry-like core–shell $BaTiO_3$-polydopamine-Ag (BT-PDA-Ag) hybrid nanocomposites were produced by Xingyi Huang et al., along with the related poly (vinylidenefluoride-co-hexafluroro propylene) P(VDF-HFP)/BT-PDA-Ag nanocomposites (Fig. 11.7). The PDA shell not only made it easier to disperse the BT nanoparticles homogeneously throughout the P (VDF-HFP) matrix, but it also improved the interfacial interaction between the polymer matrix and the nanoparticle. In order to properly introduce the Coulomb-blockade effect into the nanocomposites, the nano-Ag was painted in a homogeneous manner onto the PDA shell. In comparison with P (VDF-HFP)/BT-PDA and P (VDF-HFP)/BT, the polymer matrix with BT-PDA-Ag displays exceptional electric properties. These excellent electric properties include reduced remnant polarization, suppressed dielectric loss, enhanced energy efficiency, and energy density as well as breakdown strength. Therefore, the nanocomposites that were produced as a consequence have a great deal of promise for use in dielectric and energy storage applications. This discovery also paves the way for the development of novel methods for the preparation of nanocomposites that have a high energy density and a low dielectric loss [62].

$BaTiO_3$ nanowires with a TiO_2 shell layer encapsulation were produced by Xingyi Huang and co-workers in order to construct polymer nanocomposites with a high capacity for energy storage. According to the findings of the research, the shell

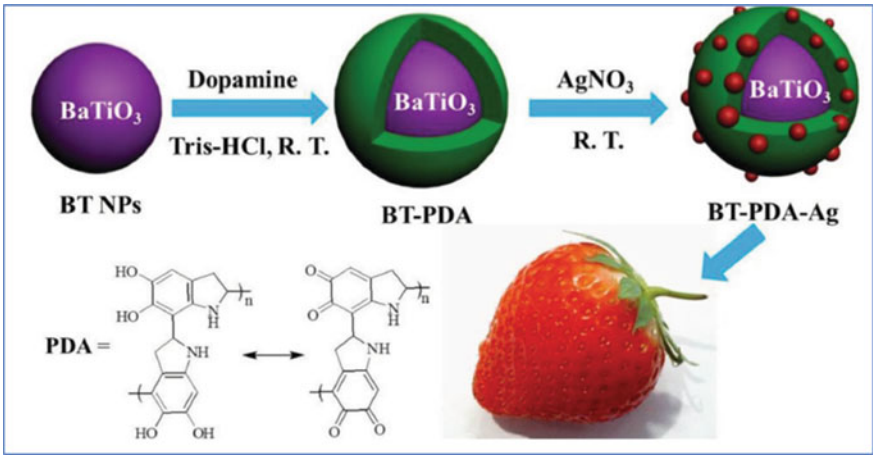

Fig. 11.7 Schematic representation of strawberry like BT-PDA-Ag nanoparticles [62]. Adopted with permission from Ref. [62] copyright@ 2015 WILEY–VCH Verlag GmbH & Co. KGaA, Weinheim

width of the buffer layer on the nanofillers plays an essential role in the process of customizing the performance of the nanocomposites that are created in this way. By using nanowires with a core–shell structure rather than bare one, it was possible to drastically reduce both the dielectric loss and the leakage current. Additionally, the introduction of TiO_2 shell layers helped to improve the reduction in the breakdown strength of these nanocomposites that included raw nanowires. The decrease of dielectric loss and the amplification of electric fields in polymer nanocomposites was another area where the finite element analysis validated the superiority of TiO_2 shell layer-encased nanowires. In light of this fact, the nanocomposites that had TiO_2 shell layers that enclosed $BaTiO_3$ NWs demonstrated a significantly enhanced capacity for the storage of energy in contrast to those that contained naked nanowires. The extensive analysis of the core–shell nanowires' electrical properties revealed that the performance of the nanocomposites does not rise in a linear fashion with increasing shell thickness. Instead, the performance of the nanocomposites was shown to be something that could be optimized by varying the shell thickness. This opens the door for the construction of high-energy-density polymer nanocomposites that are appropriate for use in applications involving the next generation of energy storage capacitors (Fig. 11.8) [63].

Core–shell BT@Al_2O_3 nanoparticles were developed by Yao Wanga and Yuan Deng et al., and then integrated into the PVDF matrix to generate flexible composite films. This was accomplished via a heterogeneous nucleation approach. There were discernible impacts of the uniform Al_2O_3 shell on the nanocomposite's resultant dielectric properties, and these effects were detected. The nanocomposite with bare BT NPs had a dielectric loss of about 0.02 and a conductivity of about 2.3×10^{-8} Sm^{-1}, whereas the composite with 20 vol% BT@ Al_2O_3 NPs had conductivity that was about 2.3×10^{-8} Sm^{-1}. This represents a decrease of about 48% and

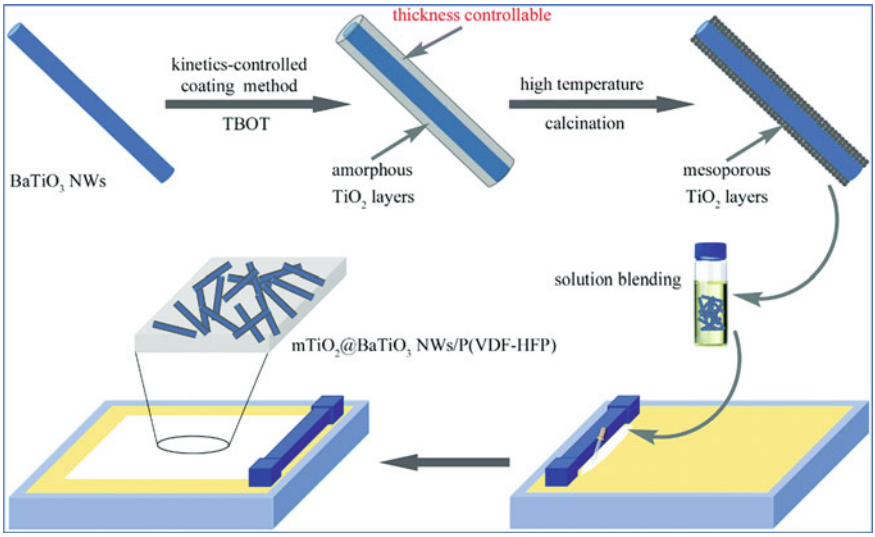

Fig. 11.8 Schematic diagram of the preparation of $mTiO_2$@$BaTiO_3$ NWs followed by synthesis of nanocomposite film [63]. Adopted with permission from Ref. [63] copyright@2017, Royal Society of Chemistry

78.8%, respectively, from the nanocomposite with bare BT NPs. The use of an Al_2O_3 shell layer has been shown to effectively reduce interfacial polarization as well as electric conduction and electric field concentration in composites. This has led to an increase in dielectric breakdown strength as well as a reduction in energy loss without causing degradation in the dielectric constant or discharged energy storage density. They revealed an efficient approach for obtaining dielectric materials with fairly low dielectric loss and decreased energy storage loss. These are extremely significant factors for assessing the performances of high-power systems, and the method demonstrates how it may be done [5] (Fig. 11.9).

Sandwiched polymer ceramic-based dielectrics were developed by Chung Ming Leung and co-workers. These dielectrics show the possibility for use in energy storage devices owing to their large power density, excellent flexibility, and cheaper cost. The poor energy storage density, however, continues to be the barrier in this process. These nanocomposite films are designed by keeping the poly (vinylidene fluoride) (PVDF) as the middle layer integrated with $BaTiO_3$ (BT) coated Ag nanomaterials (Ag@BT NPs). The bottom/top layers are composed of PVDF-embedded 2D layered MXene nanosheets. This results in the formation of sandwiched polymer-ceramic nanocomposite films. It is interesting to note that the composite best performed with a reversible energy storage density (U_eW_{re}) as high as 22.3 J/cm^3 and an efficiency of 77% at a low electric field of 270 MV/m that are reached for the film with a middle layer that contains 5 weight percent DA@Ag@BT/PVDF. The high-energy storage ability may be attributed to the strong interfacial coupling, ionic contact, and higher breakdown strength owing to the Coulomb-blockade effect in the hierarchical

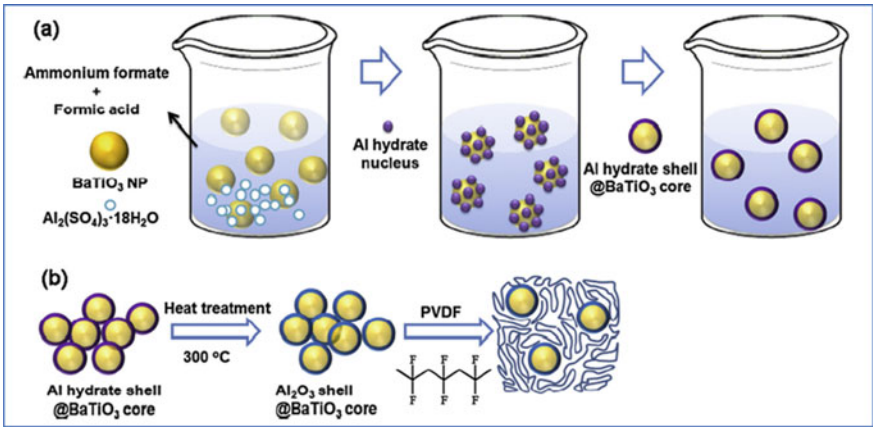

Fig. 11.9 Schematic presentation of **a** Synthesis of $BaTiO_3@Al_2O_3$ nanoparticles and **b** $BaTiO_3@Al_2O_3$/PVDF [5]. Adopted with permission from Ref. [5] copyright@ 2016, Elsevier Ltd.

structures that include a variety of fillers. In addition, the results of the phase-field simulation demonstrated that enough quantity of DA@Ag@BT NPs can effectively avoid the creation of conductive networks, suppress dielectric loss, and increase breakdown strength. This hierarchical technique offers an appropriate route for the fabrication of high-performance polymer nanocomposites (Fig. 11.10) [64].

Poly (p-phenylenebenzobisoxazole) (PBO) is a kind of polymer that maintains its structural integrity at high temperatures. However, its employment in high-performance dielectrics is limited due to its poor processability as well as its low inherent dielectric constant. Xiaoyun Liu and Qixin Zhuang produced PBO using the precursor technique, and the preparation of polymer films is carried out using solution casting, which is a more time- and labor-efficient approach than the

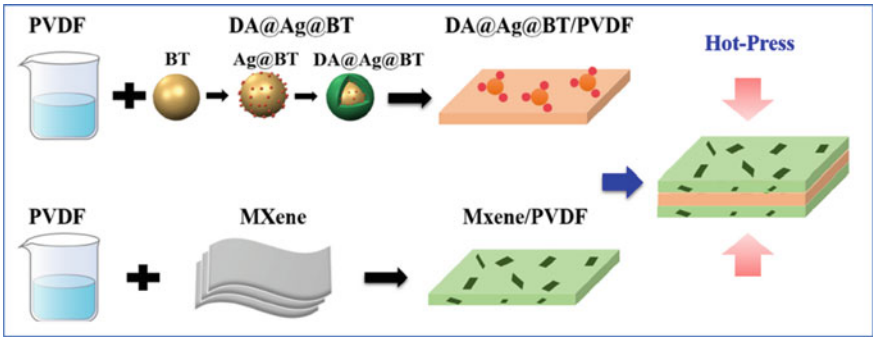

Fig. 11.10 Schematic representation of the synthesis of DA@Ag@BT, MXene, and sandwiched structure of MP-xDA@Ag@BT/PVDF [64]. Adopted with permission from Ref. [64] copyright@ 2022, Elsevier Ltd. and Techna Group S.r.l

conventional way of processing. In addition to this, a hierarchically organized one-dimensional Al_2O_3@$NaNbO_3$ is fabricated and then injected into the PBO matrix. The nanocomposite has significantly improved dielectric characteristics and breakdown strength as a result of both its high aspect ratio and its unique structure, which is Al_2O_3@$NaNbO_3$. The nanocomposite that is filled with 3 volume percent Al_2O_3@$NaNbO_3$exhibits the maximum breakdown strength of 286 kV mm^{-1}. In addition, maintains a high dielectric constant of 6.68 as well as a low dielectric loss of 0.035 at 1 kHz. Further, the energy density enhanced to 1.64 J cm^{-3} at 250 kV mm^{-1}. This is about 200% higher than the pure PBO and the nanocomposite has a low dielectric loss. In addition, the dielectric characteristics of 3 vol% Al_2O_3@$NaNbO_3$-PBO demonstrate remarkable thermal stability from 25 to 250 °C. This great thermal stability may be due to the heat resistance of both PBO and Al_2O_3@$NaNbO_3$, which are both present in the material. This study demonstrates a potentially useful method for the fabrication of polymeric dielectrics that may be used in harsh conditions [65].

In the constantly emerging areas, the synthesis of multifunctional epoxy resins using environmentally friendly processes is significant (AI, 5G, IoT, electrical and electronics appliances). In order to accomplish this goal, a multifunctional nanocomposite was manufactured by Yiting Xu et al. by utilizing electrostatic interactions and hydrogen bonding to functionalize a coating of bio-based polyelectrolyte (containing chitosan and phytate) on the surface of boron nitride in an environmentally friendly manner. This coating was done in order to create a multifunctional nanoparticle with multiple applications. Most significantly, the building process makes no use of any organic solvents and does not rely on any outside sources of heat. Further, this nanoparticle with several functions is used in the process of functionally modifying epoxy resin. The LOI value of the functionalized epoxy resin is increased to 32.8% at a reduced adding quantity of 7 weight% because of the synergistic action of polyelectrolyte and boron nitride at the nanoscale. In addition, when subjected to a vertical combustion test, the modified epoxy resin demonstrated a quick extinguishing phenomenon that lasted for just 0.5 s after the fire source was turned off. When compared with clean EP, the peak heat release rate (pHRR) and total smoke production (TSP) both show reductions of 54.3% and 33.0%, respectively. Additionally, the multifunctional nanoparticles confer excellent thermal conductivity, mechanical characteristics, and dielectric properties on the modified epoxy. Overall, the results of this study provide a sustainable approach to the production of epoxy resins with several functionalities (Fig. 11.11) [66].

Due to the high dielectric constant that may be attained around the percolation threshold, conductive filler-filled polymer composites have shown a great deal of promise. However, the substantial dielectric loss that is connected with these composites prevents their widespread use in reality. In recent years, considerable effort has been put toward encapsulating conductive fillers within an insulating shell, with the intention of limiting the dielectric loss. This conundrum begs the issue of whether or not core–shell structured fillers are ultimately useful for the dielectric performance of composites, which is an area that has received less investigation. For this purpose, Zhi-Min Dang evaluated the properties of polymer nanocomposites that include a variety

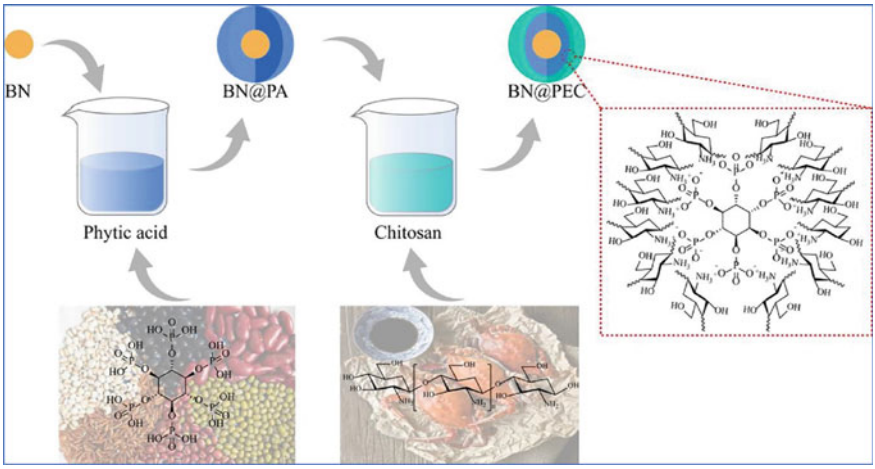

Fig. 11.11 Schematic representation of a green synthetic procedure for BN@PEC [66]. Adopted with permission from Ref. [66] copyright@ 2022, Elsevier Ltd.

of Al@Al_2O_3 nanofillers with varying shell thicknesses. It demonstrates that a rapid intra-particle polarization and a sluggish inter-particle polarization both contribute to the high dielectric constant of percolative composites. The formation of an insulating shell makes it possible to exercise separate control over the two polarizations, which, in ordinary percolative composites, would otherwise be linked (meaning that they would increase or decrease simultaneously). The core–shell structured nanocomposites are able to obtain a high dielectric constant, while simultaneously having a low dielectric loss, which is a significant improvement over the unmodified nanofiller composites. This is accomplished by promoting polarization within the particle and suppressing polarization between the particles. In addition to that, both the thermal conductivity and the high field resistivity have been increased, which brings about an operating temperature that is both consistent and low. This study presents a new paradigm for the design of percolative polymer composites, which have the potential to increase thermomechanical characteristics in addition to having a high dielectric constant and a low dielectric loss [67].

Inorganic nanoparticles with a high dielectric constant (ε_r) have been used to strengthen dielectric polymer nanocomposites, which have been the subject of much research for energy storage functions in modern electronics and electrical devices. Although the integration of inorganic nanoparticles with a high ε_r-value can enhance the ε_r-value of the composite matrix to a certain level, it will also certainly decrease the inclusive breakdown strength (E_b) of the complex matrix. This eventually hampers the effective enhancement of the energy storage efficacy of the composites. Xin Zhang et al. developed a method to fabricate high-ε_r $BaTiO_3$ (BTO) nanoparticles with polyimide polymer (PI) shells (PI@BTO) through an in situ polymerization technique using poly etherimide (PEI)-based nanocomposites. Because of the modified PI shell, the interaction between the organic or inorganic interface has

been improved, which has led to a uniform distribution of nanoparticles throughout the PEI composite matrix. Specifically, the normal electrostatic interaction between the PEI matrix and polymer chains present in the PI shell increases the E_b of the PEI/PI@BTO nanocomposite in comparison with pure PEI. This, in turn, results in a high charge–discharge efficiency (η) of more than 80% and a high-energy storage density (U_e) of 6.2 J/cm^3 in the PEI nanocomposites, which is an improvement of 150% than that of pure PEI. The work proposes a facile and efficient approach for surface functionalization to increase the compatibility between the interfaces and E_b of polymer nanocomposite matrix. Furthermore, the remarkably improved performances in energy storage of the synthesized nanocomposite matrix provide great potential for the fabrication of high-performance capacitors to meet the growing demands for more compact, energy-efficient, and cost-effective electrical device electronics[68].

Filling an organic dielectric with inorganic nanoparticles that have a high dielectric constant is an efficient method that may be used to improve the energy storage capability of the dielectric. On the other hand, the dielectric difference between polymer and ceramic produces early breakdown, which in turn restricts the storage density of ceramic/polymer nanocomposites when they are used for dielectric capacitors. Liang Cao and Huixing Lin et al. used magnesium oxide (MgO) as a buffer barrier because of its high medium dielectric constant and insulation. This was done to diminish the difference in dielectric characteristics that were present between the poly (vinylidene fluoride-hexafluoropropylene) (P (VDFHFP)) substrate and $BaTiO_3$ (BT) nanoparticles. A straightforward chemical precipitation procedure was used to coat the spherical BT with the foreign oxide, resulting in the formation of a $BaTiO_3$@MgO (BT@MgO) core–shell nanostructure. This structure has been meticulously analyzed by EDS and TEM. As a result of the BT-MgO heterogeneous interfacial region's provision of carrier channels and promotion of charge movement, both the dielectric constant and the potential shift have been greatly improved. The BT@MgO/P (VDF-HFP) nanocomposite with a filling ratio of 1 volume percent gave the greatest energy density U_d. The U_d value extends up to 5.6 J/cm^3, which is 55.6% and 40.0% larger than that of the BT-filled counterpart and host matrix with the same filler quantity. The BT@MgO core–shell nanostructure is an example of an alternate method that may effectively increase the energy storage functioning of polymer/ceramic composite dielectrics. Due to MgO's high insulation and medium dielectric constant, it has been decided to use it as a buffer barrier between the BT nanoparticles and the P (VDF-HFP) substrate in this research. This helped to reduce the dielectric mismatch that existed between the two. The core–shell $BaTiO_3$@MgO nanoparticles have a heterogeneous interfacial area that is composed of BTMgO. This region functions to create pathways for carriers and enhance charge mobility. Therefore, the inclusion of an MgO shell considerably improved the energy storage qualities. The BT@MgO-reinforced composite dielectric with a 1 volume % filling ratio achieved the highest possible U_d value for energy density. At 4235 kV/cm this value reached 5.6 J/cm^3, which is larger by 40.0% than that of the host matrix and 55.6% more than that of BT-loaded dielectric with similar filler composition. In the meanwhile, it maintains a high-energy usage efficacy, with a value of 51.3%

for the coefficient. The core–shell-structured BT@MgO nanofiller is an example of an alternate approach that may effectively enhance the energy storage function of polymer/ceramic dielectric composites [69].

11.4 Conclusion

In conclusion, this chapter discusses the various methods of preparation of high-k core–shell nanomaterials for dielectric applications. Core–shell techniques have made significant strides in enhancing nanocomposites with high-k for dielectric applications and energy storage, however, these techniques suffer from certain problems. These problems include producing high-k nanocomposites that concurrently display a low dielectric loss, high breakdown strength, and other desired features at large production scales while preserving fine control over the nanostructures of the core–shell nanoparticles. Utilizing one-core multiple-shell systems, including nanoparticles with desired nanoeffects in the shells, and developing advanced synthesis processes for core–shell nanomaterials may give technological means to transcend these limitations.

References

1. Luo S, Yu J, Yu S, Sun R, Cao L, Liao WH, Wong CP (2019) Significantly enhanced electrostatic energy storage performance of flexible polymer composites by introducing highly insulating-ferroelectric microhybrids as fillers. Adv Energy Mater 9(5):1803204
2. Wang PJ, Zhou D, Guo HH, Liu WF, Su JZ, Fu MS, Singh C, Trukhanov S, Trukhanov A (2020) Ultrahigh enhancement rate of the energy density of flexible polymer nanocomposites using core–shell $BaTiO_3$@ MgO structures as the filler. J Mater Chem A 8(22):11124–11132
3. Wang P-J, Zhou D, Li J, Pang L-X, Liu W-F, Su J-Z, Singh C, Trukhanov S, Trukhanov A (2020) Significantly enhanced electrostatic energy storage performance of P (VDF-HFP)/$BaTiO_3$-Bi (Li0. 5Nb0. 5) O3 nanocomposites. Nano Energy 78:105247
4. Zheng W, Ren L, Zhao X, Li H, Xie Z, Li Y, Wang C, Yu L, Yang L, Liao R (2022) Tuning interfacial relaxations in P(VDF-HFP) with Al_2O_3@ZrO_2 core-shell nanofillers for enhanced dielectric and energy storage performance. Compos Sci Technol 222:109379
5. He D, Wang Y, Chen X, Deng Y (2017) Core–shell structured $BaTiO_3$@Al_2O_3 nanoparticles in polymer composites for dielectric loss suppression and breakdown strength enhancement. Compos A Appl Sci Manuf 93:137–143
6. Huang X, Jiang P (2015) Core–shell structured high-k polymer nanocomposites for energy storage and dielectric applications. Adv Mater 27(3):546–554
7. Wang Y, Zhou X, Chen Q, Chu B, Zhang Q (2010) Recent development of high energy density polymers for dielectric capacitors. IEEE Trans Dielectr Electr Insul 17(4):1036–1042
8. Chen Y, Xia Y, Sun H, Smith GM, Yang D, Ma D, Carroll DL (2014) Solution-processed highly efficient alternating current-driven field-induced polymer electroluminescent devices employing high-k relaxor ferroelectric polymer dielectric. Adv Funct Mater 24(11):1501–1508
9. Ortiz RP, Facchetti A, Marks TJ (2010) High-k organic, inorganic, and hybrid dielectrics for low-voltage organic field-effect transistors. Chem Rev 110(1):205–239
10. Li J, Sun Z, Yan F (2012) Solution processable low-voltage organic thin film transistors with high-k relaxor ferroelectric polymer as gate insulator. Adv Mater 24(1):88–93

11. Kim Y-J, Kim J, Kim YS, Lee J-K (2013) Erratum to "TiO_2-poly (4-vinylphenol) nanocomposite dielectrics for organic thin film transistors. Org Electron 14:3406–3414; 2(15):640 (2014)
12. Zhang QM, Bharti V, Zhao X (1998) Giant electrostriction and relaxor ferroelectric behavior in electron-irradiated poly (vinylidene fluoride-trifluoroethylene) copolymer. Science 280(5372):2101–2104
13. Zhang Q, Li H, Poh M, Xia F, Cheng Z-Y, Xu H, Huang CJN (2002) An all-organic composite actuator material with a high dielectric constant. Nature 419(6904):284–287
14. Dang ZM, Yuan JK, Yao SH, Liao RJ (2013) Flexible nanodielectric materials with high permittivity for power energy storage. Adv Materi 25(44):6334–6365
15. Chu B, Zhou X, Ren K, Neese B, Lin M, Wang Q, Bauer F, Zhang QJS (2006) A dielectric polymer with high electric energy density and fast discharge speed. Science 313(5785):334–336
16. Alam MA, Azarian MH, Pecht MG (2012) Effects of moisture absorption on the electrical parameters of embedded capacitors with epoxy-$BaTiO_3$ nanocomposite dielectric. J Mater Sci Mater Electron 23:1504–1510
17. Dang Z-M, Yuan J-K, Zha J-W, Zhou T, Li S-T, Hu G-H (2012) Fundamentals, processes and applications of high-permittivity polymer–matrix composites. Progr Mater Sci 57(4):660–723
18. Huang X, Xie L, Yang K, Wu C, Jiang P, Li S, Wu S, Tatsumi K, Tanaka T (2014) Role of interface in highly filled epoxy/$BaTiO_3$ nanocomposites. Part I-correlation between nanoparticle surface chemistry and nanocomposite dielectric property. IEEE Trans Dielectr Electr Insul 21(2):467–479
19. Sharifi E, Jayaram SH, Cherney EA (2010) Temperature and electric field dependence of stress grading on form-wound motor coils. IEEE Trans Dielectr Electr Insul 17(1):264–270
20. Hwang SK, Bae I, Cho SM, Kim RH, Jung HJ, Park C (2013) High performance multi-level non-volatile polymer memory with solution-blended ferroelectric polymer/high-k insulators for low voltage operation. Adv Funct Mater 23(44):5484–5493
21. Arbatti M, Shan X, Cheng ZY (2007) Ceramic–polymer composites with high dielectric constant. Adv Mater 19(10):1369–1372
22. Das RN, Lauffer JM, Markovich VR (2008) Fabrication, integration and reliability of nanocomposite based embedded capacitors in microelectronics packaging. J Mater Chem 18(5):537–544
23. Li J, Seok SI, Chu B, Dogan F, Zhang Q, Wang Q (2009) Nanocomposites of ferroelectric polymers with TiO2 nanoparticles exhibiting significantly enhanced electrical energy density. Adv Mater 21(2):217–221
24. Kim P, Jones SC, Hotchkiss PJ, Haddock JN, Kippelen B, Marder SR, Perry JW (2007) Phosphonic acid-modified barium titanate polymer nanocomposites with high permittivity and dielectric strength. Adv Mater 19(7):1001–1005
25. Kim P, Doss NM, Tillotson JP, Hotchkiss PJ, Pan MJ, Marder SR, Li J, Calame JP, Perry JW (2009) High energy density nanocomposites based on surface-modified $BaTiO_3$ and a ferroelectric polymer. ACS Nano 3(9):2581–2592
26. Hu P, Shen Y, Guan Y, Zhang X, Lin Y, Zhang Q, Nan CW (2014) Topological-structure modulated polymer nanocomposites exhibiting highly enhanced dielectric strength and energy density. Adv Funct Mater 24(21):3172–3178
27. Paniagua SA, Kim Y, Henry K, Kumar R, Perry JW, Marder SR (2014) Surface-initiated polymerization from barium titanate nanoparticles for hybrid dielectric capacitors. ACS Appl Mater Interfaces 6(5):3477–3482
28. Xie L, Huang X, Wu C, Jiang P (2011) Core-shell structured poly (methyl methacrylate)/$BaTiO_3$ nanocomposites prepared by in situ atom transfer radical polymerization: a route to high dielectric constant materials with the inherent low loss of the base polymer. J Mater Chem 21(16):5897–5906
29. Yang K, Huang X, Xie L, Wu C, Jiang P, Tanaka T (2012) Core–shell structured polystyrene/BaTiO3 hybrid nanodielectrics prepared by in situ RAFT polymerization: a route to high dielectric constant and low loss materials with weak frequency dependence. Macromolecular Rapid Commun 33(22):1921–1926

30. Tchoul MN, Fillery SP, Koerner H, Drummy LF, Oyerokun FT, Mirau PA, Durstock MF, Vaia RA (2010) Assemblies of titanium dioxide-polystyrene hybrid nanoparticles for dielectric applications. Chem Mater 22(5):1749–1759
31. Maliakal A, Katz H, Cotts PM, Subramoney S, Mirau P (2005) Inorganic oxide core, polymer shell nanocomposite as a high K gate dielectric for flexible electronics applications. J Am Chem Soc 127(42):14655–14662
32. Li Z, Fredin LA, Tewari P, DiBenedetto SA, Lanagan MT, Ratner MA, Marks TJ (2010) In situ catalytic encapsulation of core-shell nanoparticles having variable shell thickness: dielectric and energy storage properties of high-permittivity metal oxide nanocomposites. Chem Mater 22(18):5154–5164
33. Jung HM, Kang JH, Yang SY, Won JC, Kim YS (2010) Barium titanate nanoparticles with diblock copolymer shielding layers for high-energy density nanocomposites. Chem Mater 22(2):450–456
34. Pang X, He Y, Jiang B, Iocozzia J, Zhao L, Guo H, Liu J, Akinc M, Bowler N, Tan XJN (2013) Block copolymer/ferroelectric nanoparticle nanocomposites. Nanoscale 5(18):8695–8702
35. Yang K, Huang X, Huang Y, Xie L, Jiang P (2013) Fluoro-polymer@ $BaTiO_3$ hybrid nanoparticles prepared via RAFT polymerization: toward ferroelectric polymer nanocomposites with high dielectric constant and low dielectric loss for energy storage application. Chem Mater 25(11):2327–2338
36. Dang ZM, You SS, Zha JW, Song HT, Li ST (2010) Effect of shell-layer thickness on dielectric properties in Ag@ TiO_2 core@ shell nanoparticles filled ferroelectric poly (vinylidene fluoride) composites. Phys Status Solidi (A) 207(3):739–742
37. Shen Y, Lin YH, Nan CW (2007) Interfacial effect on dielectric properties of polymer nanocomposites filled with core/shell-structured particles. Adv Funct Mater 17(14):2405–2410
38. Yu K, Niu Y, Bai Y, Zhou Y, Wang H (2013) Poly (vinylidene fluoride) polymer based nanocomposites with significantly reduced energy loss by filling with core-shell structured $BaTiO_3/SiO_2$ nanoparticles. Appl Phys Lett 102(10):102903
39. Xu J, Wong CP (2005) Low-loss percolative dielectric composite. Appl Phys Lett 87(8):082907
40. Wang YU, Tan DQ (2011) Computational study of filler microstructure and effective property relations in dielectric composites. J Appl Phys 109(10):104102
41. Balasubramanian B, Kraemer KL, Reding NA, Skomski R, Ducharme S, Sellmyer DJ (2010) Synthesis of monodisperse TiO_2−paraffin core−shell nanoparticles for improved dielectric properties. ACS Nano 4(4):1893–1900
42. Ducharme S (2009) An inside-out approach to storing electrostatic energy. ACS Nano 3(9):2447–2450
43. Ghosh Chaudhuri R, Paria S (2012) Core/shell nanoparticles: classes, properties, synthesis mechanisms, characterization, and applications. Chem Rev 112(4):2373–2433
44. Guo N, DiBenedetto SA, Tewari P, Lanagan MT, Ratner MA, Marks TJ (2010) Nanoparticle, size, shape, and interfacial effects on leakage current density, permittivity, and breakdown strength of metal oxide− polyolefin nanocomposites: experiment and theory. Chem Mater 22(4):1567–1578
45. Guo N, DiBenedetto SA, Kwon DK, Wang L, Russell MT, Lanagan MT, Facchetti A, Marks TJ (2007) Supported metallocene catalysis for in situ synthesis of high energy density metal oxide nanocomposites. J Am Chem Soc 129(4):766–767
46. Fredin LA, Li Z, Ratner MA, Lanagan MT, Marks TJ (2012) Enhanced energy storage and suppressed dielectric loss in oxide core–shell–polyolefin nanocomposites by moderating internal surface area and increasing shell thickness. Adv Mater 24(44):5946–5953
47. Fredin LA, Li Z, Lanagan MT, Ratner MA, Marks TJ (2013) Substantial recoverable energy storage in percolative metallic aluminum-polypropylene nanocomposites. Adv Funct Mater 23(28):3560–3569
48. Stoyanov H, Mc Carthy D, Kollosche M, Kofod G (2009) Dielectric properties and electric breakdown strength of a subpercolative composite of carbon black in thermoplastic copolymer. Appl Phys Lett 94(23):232905

49. Yang K, Huang X, Zhu M, Xie L, Tanaka T, Jiang P (2014) Combining RAFT polymerization and thiol–ene click reaction for core–shell structured polymer@ $BaTiO_3$ nanodielectrics with high dielectric constant, low dielectric loss, and high energy storage capability. ACS Appl Mater Interfaces 6(3):1812–1822
50. Pirzada B, Sabir S (2018) Polymer-based nanocomposites for significantly enhanced dielectric properties and energy storage capability. In: Polymer-based nanocomposites for energy and environmental applications. Elsevier, pp 131–183
51. Xie L, Huang X, Yang K, Li S, Jiang P (2014) "Grafting to" route to PVDF-HFP-GMA/$BaTiO_3$ nanocomposites with high dielectric constant and high thermal conductivity for energy storage and thermal management applications. J Mater Chem A 2(15):5244–5251
52. Xie L, Huang X, Huang Y, Yang K, Jiang P (2013) Core@ double-shell structured BaTiO3–polymer nanocomposites with high dielectric constant and low dielectric loss for energy storage application. J Phys Chem C 117(44):22525–22537
53. Xie L, Huang X, Huang Y, Yang K, Jiang P (2013) Core-shell structured hyperbranched aromatic polyamide/BaTiO3 hybrid filler for poly (vinylidene fluoride-trifluoroethylene-chlorofluoroethylene) nanocomposites with the dielectric constant comparable to that of percolative composites. ACS Appl Mater Interfaces 5(5):1747–1756
54. Pang X, Zhao L, Han W, Xin X, Lin Z (2013) A general and robust strategy for the synthesis of nearly monodisperse colloidal nanocrystals. Nature Nanotechnol 8(6):426–431
55. Guo HZ, Mudryk Y, Ahmad MI, Pang XC, Zhao L, Akinc M, Pecharsky VK, Bowler N, Lin ZQ, Tan X (2012) Structure evolution and dielectric behavior of polystyrene-capped barium titanate nanoparticles. J Mater Chem 22(45):23944–23951
56. Rahimabady M, Mirshekarloo MS, Yao K, Lu L (2013) Dielectric behaviors and high energy storage density of nanocomposites with core–shell $BaTiO_3$ @ TiO_2 in poly (vinylidene fluoride-hexafluoropropylene). Phys Chem Chem Phys 15(38):16242–16248
57. Shen Y, Lin Y, Li M, Nan CW (2007) High dielectric performance of polymer composite films induced by a percolating interparticle barrier layer. Adv Mater 19(10):1418–1422
58. Molberg M, Crespy D, Rupper P, Nüesch F, Månson JA, Löwe C, Opris DM (2010) High breakdown field dielectric elastomer actuators using encapsulated polyaniline as high dielectric constant filler. Adv Funct Mater 20(19):3280–3291
59. Zhu L, Wang QJM (2012) Novel ferroelectric polymers for high energy density and low loss dielectrics. Macromolecules 45(7):2937–2954
60. Balberg I (2011) Electrical transport mechanisms in three dimensional ensembles of silicon quantum dots. J Appl Phys 110(6):13
61. Xie L, Huang X, Li BW, Zhi C, Tanaka T, Jiang P (2013) Core–satellite Ag@ $BaTiO_3$ nanoassemblies for fabrication of polymer nanocomposites with high discharged energy density, high breakdown strength and low dielectric loss. Phys Chem Chem Phys 15(40):17560–17569
62. Yang K, Huang X, He J, Jiang P (2015) Strawberry-like core–shell Ag@ polydopamine@ $BaTiO_3$ hybrid nanoparticles for high-k polymer nanocomposites with high energy density and low dielectric loss. Adv Mater Interfaces 2(17):1500361
63. Wang G, Huang Y, Wang Y, Jiang P, Huang X (2017) Substantial enhancement of energy storage capability in polymer nanocomposites by encapsulation of $BaTiO_3$ NWs with variable shell thickness. Phys Chem Chem Phys 19(31):21058–21068
64. Zhu J, Wang D, Liu Z, Leung CM, Chen J, Zeng M, Lu X, Gao X, Liu J-M (2022) Superior energy storage of sandwiched PVDF films by separate introduction of core-shell Ag@BT nanoparticles and 2D MXene nanosheets. Ceram Int 48(13):19274–19282
65. Li J, Jiang J, Cheng Q, Cui Z, Liu X, Zuo P, Zhuang Q (2022) Construction of a flexible 1D core–shell Al_2O_3 @$NaNbO_3$ nanowire/poly(p-phenylene benzobisoxazole) nanocomposite with stable and enhanced dielectric properties in an ultra-wide temperature range. J Mater Chem C 10(2):716–725
66. Xia L, Wang X, Ren T, Luo L, Li D, Dai J, Xu Y, Yuan C, Zeng B, Dai L (2022) Green construction of multi-functional fire resistant epoxy resins based on boron nitride with core-shell structure. Polym Degrad Stab 203:110059

67. Cheng S, Zhou Y, Li Y, Yuan C, Yang M, Fu J, Hu J, He J, Li Q (2021) Polymer dielectrics sandwiched by medium-dielectric-constant nanoscale deposition layers for high-temperature capacitive energy storage. Energy Storage Mater 42:445–453
68. Zeng J, Yan J, Li B-W, Zhang X (2022) Improved breakdown strength and energy storage performances of PEI-based nanocomposite with core-shell structured PI@$BaTiO_3$ nanofillers. Ceram Int 48(14):20526–20533
69. Chen J, Huang F, Zhang C, Meng F, Cao L, Lin H (2022) Enhanced energy storage density in poly(vinylidene fluoride-hexafluoropropylene) nanocomposites by filling with core-shell structured $BaTiO_3$@MgO nanoparticals. J Energy Storage 53:105163